Synthesis and Structure of a New Ternary Chalcogenide $Nb_3Pd_{0.72}Se_7$; Interrelationships in the Packing of Prisms and Planes

Douglas A. Keszler and James A. Ibers*

Contribution from the Department of Chemistry, Northwestern University, Evanston, Illinois 60201. *Received April 8, 1985*

Abstract: The ternary chalcogenide $Nb_3Pd_{0.72}Se_7$ has been synthesized and its structure has been established through single-crystal X-ray measurements. The compound crystallizes in space group C_{2h}^3—$C2/m$ of the monoclinic system with four formula units in a cell of dimensions a = 12.803 (2) Å, b = 3.413 (1) Å, c = 21.058 (2) Å, and β = 95.47 (1)°. The structure is a new laminar type that consists of layers of formula $^2_\infty[Nb_6PdSe_{14}]$. Between these layers additional Pd atoms statistically occupy (43%) a rhombic site. Occurrence of the layers $^2_\infty[Nb_6PdSe_{14}]$ and the known layers $^2_\infty[Nb_4PdSe_{10}]$ and $^2_\infty[Nb_2PdSe_6]$ allows formulation of the set of layers $^2_\infty[Nb_{2n}PdSe_{4n+2}]$, where n = 1, 2, and 3 have thus far been observed. This formulation includes the compositional behavior as well as the structural pattern that evolves with a serial change in the index n. This structural pattern is extended with comparisons between this set and the structural types $NbSe_3$, $NbSe_2$, $Nb_2Pd_3Se_8$, and $Co_2Ta_4PdSe_{12}$. From these comparisons, structural details, valence descriptions, and physical properties a model for the electronic structure of the ternary phases that contain Nb, Pd, and Se atoms is proposed.

Introduction

A variety of solid-state inorganic transition-metal chalcogenides have been extensively studied during the past decade. The materials investigated have ranged from metal-rich compounds such as $SnMo_6S_8$[1] and $Tl_2Mo_6Se_6$[2] to layered phases such as $NbSe_2$,[3] $NbSe_3$,[4] and MoS_2.[5] Study of these materials has been motivated by a general utilitarian interest, an assortment of unusual structural features, and a bevy of fascinating physical properties. Among these properties are anisotropic electrical conductivity,[6] superconductivity,[7] intercalation chemistry,[8] catalysis,[9] lubricant behavior,[10] charge density waves,[11] and unusual photoelectrochemical behavior.[12]

As with any molecular or chemical assemblage, the physical properties of the transition-metal chalcogenides arise from the peculiar association of their crystal and electronic structures. In particular, many of the properties of these materials derive from metal-to-metal interactions. New and perhaps unusual properties may be anticipated to result from the preparation and study of chalcogenides having totally new structures in which unusual metallic environments are formed. Motivated in part by our desire to synthesize such transition-metal chalcogenides, we have examined the systems Nb(Ta)/Pd/Se(S) for new compounds, as we anticipated correctly that new structures would result from association of the preferred coordination geometries of these atoms.[13]

In this report we describe and compare the new phases that we have prepared. First, the synthesis and characterization of the new laminar material $Nb_3Pd_{0.72}Se_7$ is described. We then show that this material in conjunction with other layered phases from the system Nb/Pd/Se form a set of structurally similar materials. The relationships of this set with other chalcogenides that contain Pd and Nb atoms and other well-studied layered transition-metal chalcogenides are also examined.

We have previously shown[13] that the electrical conductivity of the materials from the system Nb(Ta)/Pd/Se(S) ranges from semiconducting to metallic. These observations and the interrelationships developed here provide a simple understanding of the electronic characteristics of these materials.

Experimental Section

Synthesis of $Nb_3Pd_{0.72}Se_7$. The crystal of the phase $Nb_3Pd_{0.72}Se_7$ used in the single-crystal X-ray study (vide infra) was prepared from a reaction of the elements combined in the ratio Nb:Pd:Se, 4:1:10 (Nb powder, 99.9%, AESAR; Pd powder, 99.9%, AESAR; Se powder, 99.999%, Atomergic). The metals Nb and Pd were reduced under a flow of H_2 at 875 K for 4 h prior to reaction. The elements were loaded into a silica tube that was then evacuated to $\sim 10^{-6}$ torr. The tube was sealed and placed in a tube furnace that was heated from 300 to 725 K at 15 deg/h. After being heated to the maximum temperature and then radiatively

(1) (a) Espelund, A. *Acta Chem. Scand.* **1967**, *21*, 839–841. (b) Chevrel, R.; Sergent, M.; Prigent, J. *J. Solid State Chem.* **1971**, *3*, 515–519. (c) Fischer, Ø.; Odermatt, R.; Bongi, G.; Jones, H.; Chevrel, R.; Sergent, M. *Phys. Lett. A* **1973**, *45*, 87–88. (d) Delk, F. S., II; Sienko, M. J. *Inorg. Chem.* **1980**, *19*, 788–789. (e) Hinks, D. G.; Jorgensen, J. D.; Li, H. C. *Phys. Rev. Lett.* **1983**, *51*, 1911–1914. (f) Miller, W. M.; Ginsberg, D. M. *Phys. Rev. B: Condens. Matter* **1983**, *28*, 3765–3769. (g) Hinks, D. G.; Jorgensen, J. D.; Li, H. C. *Solid State Commun.* **1984**, *49*, 51–54.

(2) (a) Potel, M.; Chevrel, R.; Sergent, M. *Acta Crystallogr. B* **1980**, *36*, 1545–1548. (b) Potel, M.; Chevrel, R.; Sergent, M. *J. Solid State Chem.* **1980**, *35*, 286–290. (c) Hughbanks, T.; Hoffmann, R. *J. Am. Chem. Soc.* **1983**, *105*, 1150–1162. (d) Hughbanks, T.; Hoffmann, R. *Inorg. Chem.* **1982**, *21*, 3578–3580.

(3) (a) Brown, B. E.; Beernsten, D. *Acta Crystallogr.* **1965**, *18*, 31–36. (b) Marezio, M.; Dernier, P. D.; Menth, A.; Hull, G. W., Jr. *J. Solid State Chem.* **1972**, *4*, 425–429. (c) Parkin, S. S. P.; Friend, R. H. *Philos. Mag. B* **1980**, *41*, 65–94. (d) Parkin, S. S. P.; Philos. *Mag. B* **1980**, *42*, 627–642. (e) Mutka, H. *Phys. Rev. B; Condens. Matter* **1981**, *28*, 2855–2858. (f) Chen, C. H. *Solid State Commun.* **1984**, *49*, 645–647.

(4) (a) Hodeau, J. L.; Marezio, M.; Roucau, C.; Ayroles, R.; Meerschaut, A.; Rouxel, J.; Monceau, P. *J. Phys. C* **1978**, *11*, 4117–4134. (b) Monceau, P. *Solid State Commun.* **1977**, *24*, 331–334. (c) Fleming, R. M.; Polo, J. A., Jr.; Coleman, R. V. *Phys. Rev. B* **1978**, *17*, 1634–1644. (d) Chaussy, J.; Haen, P.; Lasjaunias, P.; Monceau, P.; Waysand, G.; Waintal, A.; Meerschaut, A.; Molinié, P.; Rouxel, J. *Solid State Commun.* **1976**, *20*, 759–763. (e) Molinié, P.; Meerschaut, A.; Rouxel, J.; Monceau, P.; Haen, P. *Nouv. J. Chim.* **1977**, *1*, 205–209. (f) Monceau, P.; Ong, N. P.; Portis, A. M.; Meerschaut, A.; Rouxel, J. *Phys. Rev. Lett.* **1976**, *37*, 602–606. (g) Dee, R. H.; Chaikin, P. M.; Ong, N. P. *Phys. Rev. Lett.* **1979**, *42*, 1234–1237. (h) Onuki, Y.; Inada, R.; Tanuma, S.; Yamanaka, S.; Kamimura, H. *Solid State Ionics* **1983**, *11*, 195–201. (i) Chen, C. H.; Fleming, R. *Phys. Rev. B: Condens. Matter* **1984**, *29*, 4811–4813. (j) Everson, M. P.; Eiserman, G.; Johnson, A.; Coleman, R. V. *Phys. Rev. Lett.* **1984**, *52*, 1721–1724. (k) Meerschaut, A.; Rijnsdorp, J.; Folmer, J. C. W.; Jellinek, F. *Stud. Inorg. Chem.* **1983**, *3*, 777–780. (l) Yamayo, K.; Oomi, G. *J. Phys. Soc. Jpn.* **1983**, *52*, 1886–1887. (m) Cedzynska, K.; Parker, A. J.; Singh, P. *J. Power Sources* **1983**, *10*, 13–21.

(5) (a) Dickinson, R. G.; Pauling, L. *J. Am. Chem. Soc.* **1923**, *45*, 1466–1471. (b) Schneemeyer, L. F.; Cohen, U. *J. Electrochem. Soc.* **1983**, *130*, 1536–1539. (c) Huntley, D. R.; Parham, T. G.; Merrill, R. P.; Sienko, M. J. *Inorg. Chem.* **1983**, *22*, 4144–4146. (d) Chianelli, R. R.; Percoraro, T. A.; Halbert, T. R.; Pan, W. H.; Stiefel, E. I. *J. Catal.* **1984**, *86*, 226–230.

(6) Wilson, J. A.; Yoffe, A. D. *Adv. Phys.* **1969**, *18*, 193–335.

(7) (a) Matthias, B. T.; Marezio, M.; Corenzwit, E.; Cooper, A. S.; Barz, H. E. *Science* **1972**, *175*, 1465–1466. (b) Mato, Y.; Toyota, N.; Noto, K.; Hoshi, A. *Phys. Lett. A* **1973**, *45*, 99–100.

(8) Whittingham, M. S. *Prog. Solid State Chem.* **1978**, *12*, 41–125.

(9) (a) Grange, P.; Delmon, B. *J. Less-Common Met.* **1974**, *36*, 353–360. (b) Pecoraro, T. A.; Chianelli, R. *J. Catal.* **1981**, *67*, 430–445.

(10) (a) Church, D. *Molybdenum Mosaic* **1982**, *5*, 8–12. (b) Sliney, H. E. *Tribol. Int.* **1982**, *15*, 303–315.

(11) Di Salvo, F. J. *Surf. Sci.* **1976**, *58*, 297–311.

(12) Tributsch, H. *Struct. Bonding* **1982**, *49*, 127–182.

(13) (a) Keszler, D. A.; Ibers, J. A. *J. Solid State Chem.* **1984**, *52*, 73–79. (b) Keszler, D. A.; Ibers, J. A.; Shang, M.; Lu, J. *J. Solid State Chem.* **1985**, *57*, 68–81. (c) Keszler, D. A.; Squattrito, P. J.; Brese, N. E.; Ibers, J. A.; Shang, M.; Lu, J. *Inorg. Chem.* **1985**, *24*, 3063–3067.

0002-7863/85/1507-8119$01.50/0

Table I. Crystal Data and Intensity Collection for $Nb_3Pd_{0.72}Se_7$

mol wt, amu	906.98
space group	C_{2h}^3—C2/m
a, Å	12.803 (2)
b, Å	3.413 (1)
c, Å	21.058 (2)
β,[a] deg	95.47 (1)
V, Å^3	916
Z	4
T of data collection, K	298
radiation	graphite monochromatized Mo Kα (λ(Kα_1) = 0.7093 Å)
crystal shape	Rod, bound by faces of the forms {010}, {20$\bar{1}$}, {100}; ca. 0.02 × 0.39 × 0.008
crystal vol, mm^3	6.7×10^{-5}
linear abs coeff, cm^{-1}	323
transmission factors[b]	0.472–0.782
detector aperture, mm	horizontal slit, 3; vertical slit, 2.0 + 1.25 tan θ, 20 cm from crystal
takeoff angle, deg	2.6
scan speed,[c] deg min^{-1}	2.0 in ω
scan range, deg	−0.7° to +0.7° in ω
background	$^1/_4$ of scan range on each side of reflection
λ^{-1} sin θ, limits, Å^{-1}	0.0369–0.8680; 3° ≤ 2θ ≤ 76°
data collected	$\pm h,\pm k,\pm l$ (3° ≤ 2θ ≤ 42°) $\pm h,k,l$ (42° < 2θ ≤ 76°)
no. of unique data (including $F_o^2 < 0$)	2793
no. unique data with $F_o^2 > 3\sigma(F_o^2)$	1126
$R(F^2)$	0.124
$R_w(F^2)$	0.143
R (on F for $F_o^2 > 3\sigma(F_o^2)$)	0.052
error in observation of unit wt, e^2	1.14

[a] α and γ were constrained to be 90° in the refinement of cell constants. [b] The analytical method as employed in the Northwestern absorption program AGNOST was used for the absorption correction (de Meulenaer, J.; Tompa, H. *Acta Crystallogr.* **1965**, *19*, 1014–1018). [c] Reflections with $I < 2.5\sigma(I)$ were rescanned up to 120 s in an attempt to obtain $I \geq 2.5\sigma(I)$.

cooled, the tube was removed from the furnace. The charge was thoroughly ground under a dinitrogen atmosphere and passed through a 270-mesh sieve. It was then placed in a fresh silica tube and heated at 1125 K for 288 h. After 48 h of this treatment the tube was cooled, shaken vigorously, and heated again at 1125 K. At the completion of the final heating and cooling cycle small rod-shaped crystals up to 2 mm in length were dispersed in the tube. These crystals displayed a metallic luster. A chemical analysis, performed with the electron microprobe of an EDAX-equipped Cambridge S-4 scanning electron microscope, of six crystals selected at random afforded the composition $Nb_{3.02(2)}Pd_{0.73(4)}Se_{6.98(2)}$. As deduced from refinement of the X-ray data, the composition of the single crystal used in the structure determination is $Nb_3Pd_{0.716(4)}Se_7$, comparing well with that afforded by the microprobe analysis. Since the final composition as compared with the initial ratio of the reactants has a deficiency of Se atoms, excess Se must be present in the product. During the reaction this Se, serving as a mineralizer, probably assisted in the growth of the crystals. Given the satisfactory comparison between the initial and final compositions exclusive of the Se concentration, the random selection of crystals for analysis, and the synthetic procedure undertaken to ensure homogeneity, we believe the stated formula represents, within the limits of error, the equilibrium phase under these experimental conditions.

X-ray Crystallography of $Nb_3Pd_{0.72}Se_7$. Examination of the material by X-ray Weissenberg photography established that it belongs to the monoclinic system. No reflections indicative of a superstructure were observed on precession photographs obtained with Cu radiation and exposure times of 96 h. The systematic absence (hkl, $h + k = 2n + 1$) is consistent with the space groups C_{2h}^3—$C2/m$, C_s^3—Cm, and C_2^3—$C2$. We favor the centrosymmetric space group C_{2h}^3—C2/m as a satisfactory residual ($R = 2.9\%$) results from averaging all members of the form $\{hkl\}$ from the inner sphere (2θ (Mo Kα_1) ≤ 42°) of absorption-corrected data. The lattice constants were determined by a least-squares analysis of the setting angles of 25 reflections in the range 34° ≤ 2θ (Mo Kα) ≤ 40° that had been automatically centered on an Enraf-Nonius CAD4 diffractometer. As opposed to the software supplied by Enraf-Nonius this analysis takes due cognizance of the constraints $\alpha = \gamma = 90°$. The

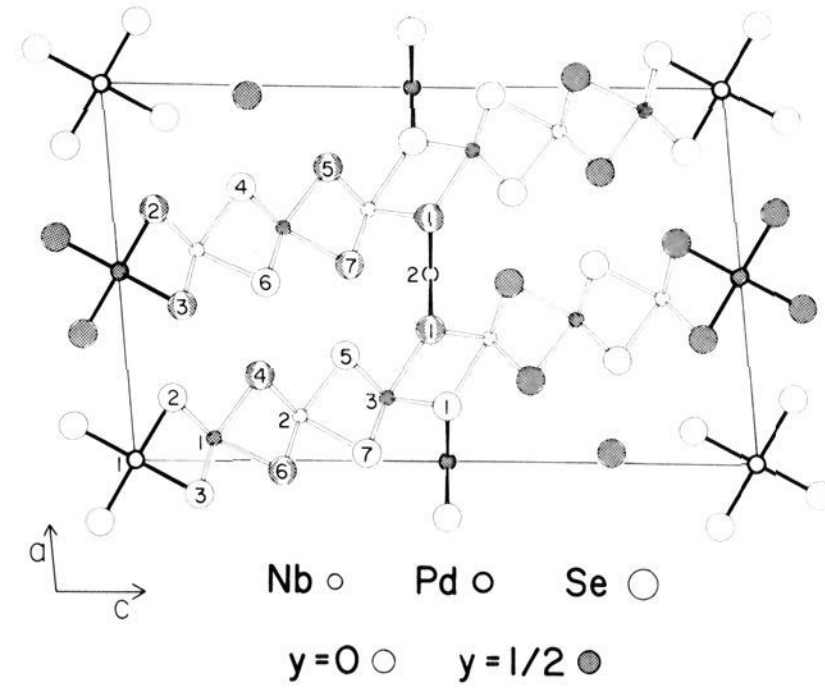

Figure 1. Projection of the structure of the phase $Nb_3Pd_{0.72}Se_7$ onto the a–c plane. The labeling scheme is shown.

refined cell constants and additional relevant crystal data are given in Table I.

Intensity data were collected with the ω-scan technique in such a manner as to force a final scan so that no reflections were termed weak and were rejected. The intensities of six standard reflections, measured every 3 h throughout data collection, were stable.

The structure was solved and refined by methods standard in this laboratory.[14] The positions of the metal atoms and the atoms Se(1) and Se(3) were determined from a Patterson synthesis. The remaining atoms were located from ensuing electron density syntheses coupled with a portion of trial and error. Scattering factors and anomalous dispersion terms were taken from the usual sources.[15] In preparation for the absorption correction the occupancy of the Pd(2) site and an isotropic thermal parameter for each atom were varied during initial cycles of full-matrix least-squares refinement performed on $|F_o|$ for $F_o^2 \geq 3\sigma(F_o^2)$. The final cycle of refinement was performed on F_o^2 and was based on all 2793 unique data and 71 variables. Included in these variables were anisotropic thermal parameters for each atom and the occupancy for atom Pd(2). The final values of R and R_w on F_o^2 are 0.124 and 0.143, respectively. The value of the conventional R index on F for those 1126 reflections having $F_o^2 > 3\sigma(F_o^2)$ is 0.052. The final difference electron density map contains no features greater than 3% of the height of a Pd atom. Analysis of F_o^2 vs. F_c^2 as a function of F_o^2, λ^{-1} sin θ, and Miller indices reveals no unusual trends.

Final atomic parameters appear in Table II. Anisotropic thermal parameters and structure amplitudes are given in Tables III and IV, respectively.[16] The anisotropic thermal parameters are unexceptional, consistent with no disorder between Nb and Pd sites.

The Structure of $Nb_3Pd_{0.72}Se_7$

A projection of the structure of the phase $Nb_3Pd_{0.72}Se_7$ with the labeling scheme appears in Figure 1. The structure is a new laminar type that consists of sheets of composition $^2_\infty[Nb_6PdSe_{14}]$[17] contiguous with the plane (20$\bar{1}$). For descriptive purposes, it is convenient to view these sheets as being built from a simpler fundamental unit. This unit $^1_\infty[Nb_6PdSe_{14}]$ is shown in Figure 2a. Here the view is orthogonal to the plane (20$\bar{1}$) and onto a section of a single layer. The unit is a combination of chains of square-planar and trigonal-prismatic Se polyhedra that are approximately centered by Pd and Nb atoms, respectively; each chain extends along the direction [010] and is occupied by only one crystallographic type of metal atom. The Pd(1) atoms center a column of face-to-face square planes. Atoms Nb(1) and Nb(2) occupy chains of edge-sharing trigonal prisms whereas atoms Nb(3) occupy columns of trigonal prisms sharing their triangular faces. These cyrstallographically independent chains associate to form the unit in a manner such that the polyhedra of adjacent

(14) See, for example: Waters, J. M.; Ibers, J. A. *Inorg. Chem.* **1977**, *16*, 3273–3277.

(15) Cromer, D. T.; Waber, J. T. "International Tables for X-ray Crystallography"; Kynoch Press: Birmingham, England, 1974; Vol. IV, Table 2.2A, pp 71–98.

(16) See paragraph at the end of the paper regarding supplementary material.

(17) The nomenclature $^n_\infty[\,]$ defines an n-dimensional extended structure.

Table II. Positional Parameters and Equivalent Isotropic Thermal Parameters for $Nb_3Pd_{0.72}Se_7$

atom	Wyckoff notation	site symmetry	x	y	z	B_{eq} (Å^2)
Pd(1)	2a	2/m	0	0	0	0.88 (4)
Pd(2)[a]	2d	2/m	0	1/2	1/2	0.90 (10)
Nb(1)	4i	m	0.059 30 (11)	1/2	0.127 824 (65)	0.81 (3)
Nb(2)	4i	m	0.117 12 (11)	0	0.269 605 (65)	0.66 (3)
Nb(3)	4i	m	0.168 51 (11)	1/2	0.411 657 (61)	0.54 (3)
Se(1)	4i	m	0.351 91 (12)	1/2	0.492 851 (71)	0.61 (3)
Se(2)	4i	m	0.166 85 (13)	0	0.067 514 (73)	0.78 (3)
Se(3)	4i	m	0.410 81 (13)	1/2	0.097 201 (72)	0.77 (3)
Se(4)	4i	m	0.225 12 (12)	1/2	0.209 658 (72)	0.64 (3)
Se(5)	4i	m	0.280 59 (12)	0	0.353 053 (70)	0.59 (3)
Se(6)	4i	m	0.471 53 (13)	0	0.233 800 (73)	0.66 (3)
Se(7)	4i	m	0.022 27 (12)	0	0.372 451 (70)	0.60 (3)

[a] Occupancy = 0.432 (8).

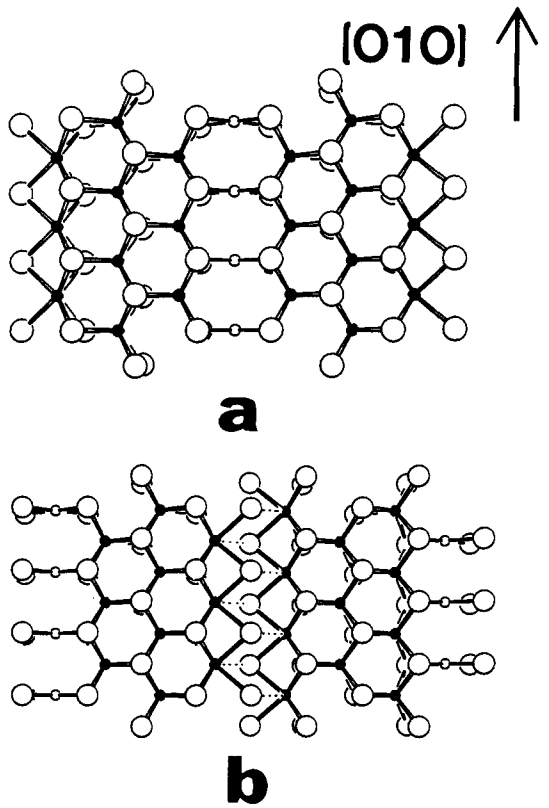

Figure 2. (a) A unit $^1_\infty[Nb_6PdSe_{14}]$; (b) juxtaposed units $^1_\infty[Nb_6PdSe_{14}]$. Both are viewed orthogonal to (20$\bar{1}$). Nb atoms are small filled circles; Pd atoms are small open circles; Se atoms are large open circles.

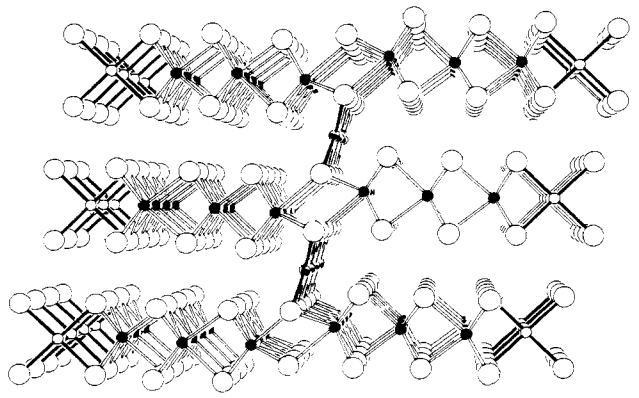

Figure 3. Perspective drawing of the phase $Nb_3Pd_{0.72}Se_7$ along the direction [010]. Nb atoms are small filled circles; Pd atoms are small open circles; Se atoms are large open circles.

columns share only edges. As depicted in Figure 2b the units $^1_\infty[Nb_6PdSe_{14}]$ then collocate through the Nb(3)-centered chain by a relative displacement of $b/2$ to form the layers $^2_\infty[Nb_6PdSe_{14}]$. This juxtaposition affords a seven-coordinate, monocapped, trigonal-prismatic environment about the metal atom Nb(3). As shown in Figure 3, the full three-dimensional nature of the structure is realized by stacking the layers in an essentially close-packed manner. This packing results in several types of interstitial sites between the layers. In the present material atom Pd(2) statistically occupies (43.2 (8)%) a rhombic site between the layers to form four coplanar bonds with atom Se(1). Hence, a broken ribbon of edge-shared square planes is formed along the direction [010] (Figure 3).

Table V. Selected Bond Distances (Å), Angles (deg), and Intralayer Se–Se Distances (Å) for $Nb_3Pd_{0.72}Se_7$

Pd(1)–2Se(3)	2.437 (2)	Se(2)–Se(3)	3.395 (2)
Pd(1)–2Se(2)	2.451 (2)	Se(2)–2Se(2)	3.413 (1)
Pd(1)–Pd(1)	3.413 (1)	Se(2)–2Se(4)	3.464 (2)
Pd(1)–4Nb(1)	3.216 (1)	Se(2)–Se(3)	3.516 (2)
Pd(2)–4Se(1)	2.545 (1)		
		Se(3)–2Se(6)	3.371 (2)
Nb(1)–2Se(3)	2.590 (2)	Se(3)–Se(2)	3.395 (2)
Nb(1)–Se(6)	2.593 (2)	Se(3)–2Se(3)	3.413 (1)
Nb(1)–2Se(2)	2.599 (2)	Se(3)–Se(2)	3.516 (2)
Nb(1)–Se(4)	2.604 (2)		
Nb(1)–2Nb(1)	3.413 (1)	Se(4)–Se(6)	3.334 (2)
Nb(1)–2Nb(2)	3.457 (2)	Se(4)–2Se(4)	3.413 (1)
		Se(4)–2Se(2)	3.464 (2)
Nb(2)–Se(7)	2.582 (2)	Se(4)–2Se(5)	3.482 (2)
Nb(2)–2Se(6)	2.586 (2)		
Nb(2)–2Se(4)	2.598 (2)	Se(5)–Se(7)	3.371 (2)
Nb(2)–Se(5)	2.602 (2)	Se(5)–2Se(5)	3.413 (1)
Nb(2)–2Nb(2)	3.413 (1)	Se(5)–2Se(1)	3.450 (2)
Nb(2)–2Nb(3)	3.452 (2)	Se(5)–2Se(4)	3.482 (2)
Nb(3)–2Se(7)	2.609 (2)	Se(6)–Se(4)	3.334 (2)
Nb(3)–2Se(5)	2.614 (2)	Se(6)–2Se(3)	3.371 (2)
Nb(3)–2Se(1)	2.669 (2)	Se(6)–2Se(7)	3.391 (2)
Nb(3)–Se(1)	2.770 (2)	Se(6)–2Se(6)	3.413 (1)
Nb(3)–2Nb(3)	3.413 (1)		
		Se(7)–Se(1)	3.126 (2)
Se(1)–2Se(1)	3.156 (3)	Se(7)–Se(5)	3.371 (2)
Se(1)–2Se(1)	3.413 (1)	Se(7)–2Se(6)	3.391 (2)
Se(1)–2Se(5)	3.450 (2)	Se(7)–2Se(7)	3.413 (1)
Se(1)–Se(7)	3.499 (2)	Se(7)–Se(1)	3.499 (2)
Se(2)–Pd(1)–Se(3)	88.00 (5)	Se(4)–Nb(2)–Se(4)	82.11 (6)
		Se(4)–Nb(2)–Se(5)	84.09 (6)
Se(1)–Pd(2)–Se(1)	84.23 (5)	Se(4)–Nb(2)–Se(6)	80.05 (5)
		Se(5)–Nb(2)–Se(7)	81.13 (7)
Se(2)–Nb(1)–Se(2)	82.08 (7)	Se(6)–Nb(2)–Se(6)	82.58 (7)
Se(2)–Nb(1)–Se(3)	81.74 (5)	Se(6)–Nb(2)–Se(7)	82.01 (6)
Se(2)–Nb(1)–Se(4)	83.50 (6)		
Se(3)–Nb(1)–Se(3)	82.42 (7)	Se(1)–Nb(3)–Se(1)	79.49 (5)
Se(3)–Nb(1)–Se(6)	81.15 (6)	Se(1)–Nb(3)–Se(5)	79.64 (5)
Se(4)–Nb(1)–Se(6)	79.82 (7)	Se(1)–Nb(3)–Se(7)	72.62 (5)
		Se(5)–Nb(3)–Se(5)	81.52 (6)
		Se(5)–Nb(3)–Se(7)	80.40 (5)
		Se(7)–Nb(3)–Se(7)	81.72 (6)
		Se(1)–Nb(3)–Se(5)	92.06 (4)
		Se(1)–Nb(3)–Se(1)	70.92 (5)

Selected bond distances and angles are given in Table V. The Pd(1)–Se distances and the Nb(1,2)–Se distances are consistent with similar lengths in the materials PdSe,[18] $Nb_2Pd_3Se_8$[13a], $Nb_2Pd_{0.71}Se_5$[13c], $NbSe_2$[3], and $NbSe_3$.[4] The long Pd(2)–Se(1) distance, 2.544 (1) Å, reflects the partial occupancy of the rhomb by atom Pd(2). The Nb(3)–Se(1) distance, 2.669 (2) Å, within the trigonal prism is longer than the other intraprism distances Nb(3)–Se(7), 2.608 (2) Å, and Nb(3)–Se(5), 2.614 (2) Å. These distances are entirely consistent with the corresponding distances 2.662 (1), 2.600 (1), and 2.612 (1) Å observed in the material $Nb_2Pd_{0.71}Se_5$.[13c] Similarly, the Nb(3)–Se(1) capping distance, 2.769 (2) Å, agrees well with that observed in $Nb_2Pd_{0.71}Se_5$, 2.766 (1) Å, and with similar interactions in the phase $NbSe_3$, 2.726 (4)–2.949 (4) Å.

In contrast to the expected metrical details for the metal-to-selenium distances, it is the aforementioned association and arrangement of polyhedra within the layers that is exceptional. This ordering affords a distance of greater than 21 Å between each of the crystallographically equivalent Pd-centered square-planar columns in which occur a variety of new and distinct metallic environments about the Nb and Pd atoms. Each Nb(3) atom has four Nb atoms as nearest metallic neighbors; there are two Nb(3) atoms and two Nb(2) atoms located at 3.413 (1) and 3.452 (2) Å, respectively. Each Nb(2) atom is adjacent to six Nb atoms that are at the vertices of a distorted hexagon; there are two each of atoms Nb(1), Nb(2), and Nb(3) located at distances 3.457 (2), 3.413 (1), and 3.452 (2) Å, respectively. The metallic environment of Nb(1) having 6 metal atoms—4 Nb atoms and 2 Pd atoms—is similar. From atom Nb(1) two Nb(2) atoms are located at 3.457 (2) Å, two Nb(1) atoms at 3.413 (1) Å, and two Pd(1) atoms at 3.216 (1) Å. The final distance, between atoms Nb(1) and Pd(1), is the shortest metal-to-metal distance in the material. The environment of atom Pd(1) consists of four Nb(1) atoms located at 3.216 (1) Å and two additional Pd(1) atoms located at 3.413 (1) Å.

All the intralayer Se···Se distances in this structure are greater than 3.12 Å. Hence there is no indication of Se–Se bonding. With the exception of atom Se(1), each of the Se atoms is bound to three metal atoms. Atom Se(1) is bound to three Nb atoms and the Pd(2) atoms that statistically occupy the rhomb between the layers.

The partial occupancy of the rhombic site by atom Pd(2) is intriguing. In this site atom Pd(2) is bound to only one of the crystallographically independent Se atoms (Se(1)). This selective occupancy affords the potential for modification of the electron count of the system by varying the concentration of atom Pd(2) while directly affecting the bonding of only one Se atom. The present extent of occupancy (43.2 (8)%) provides an additional example (cf. $Nb_2Pd_{0.71}Se_5$[13c]) of nonstoichiometry that prior to our study of the systems Nb(Ta)/Pd/Se(S) was unknown in the chemistry of Pd chalcogenides.

Structural Interrelationships. Previously we have described several new chalcogenides that contain Nb(Ta) and Pd atoms and that are structurally similar to the phase $Nb_3Pd_{0.72}Se_7$. These materials include the structural types Ta_2PdSe_6,[13b] $Nb_2Pd_{0.71}Se_5$[13c], $Nb_2Pd_3Se_8$,[13a] and $Co_2Ta_4PdSe_{12}$.[13c] A unique assemblage of metal-centered polyhedra occurs in each of these structural types. In this section we illustrate these assemblages to establish the structural similarities among them and further to provide a basis for understanding their interrelationships with other well-studied layered chalcogenides.

Although packing considerations are commonly used for the description and classification of extended inorganic structures, we prefer a description in terms of polyhedral association, as this reflects and guides our synthetic endeavors. Our approach has been to utilize the stereochemical preferences of transition metals, as exhibited in various molecular and solid-state compounds, for the preparation of new extended structures. These new compounds may then simply be viewed as an association of certain fragments

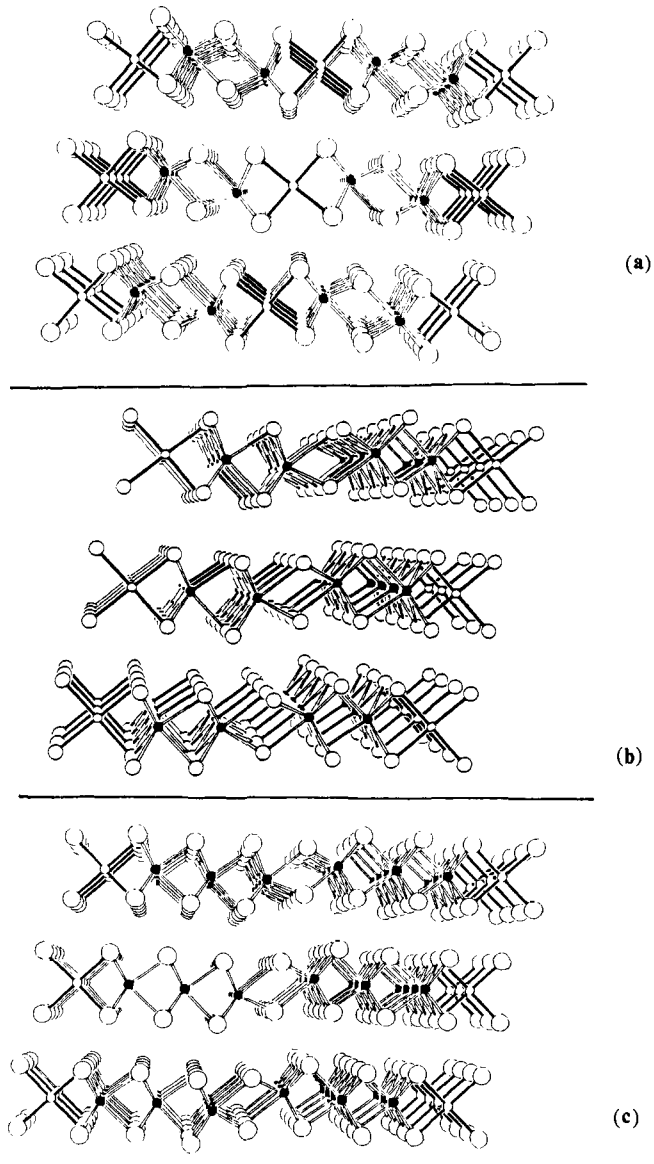

Figure 4. Perspective views of the layers (a) $^2_\infty[Nb_2PdSe_6]$, (b) $^2_\infty[Nb_4PdSe_{10}]$, and (c) $^2_\infty[Nb_6PdSe_{14}]$.

or molecules that are additionally related by translational symmetry. As the electronic structures of the individual fragments are reasonably well understood, the description also provides a convenient point for initializing a characterization of the electronic structure of the solid-state materials.

We consider first the layers of composition $^2_\infty[Nb_2PdSe_6]$, $^2_\infty[Nb_4PdSe_{10}]$, and $^2_\infty[Nb_6PdSe_{14}]$ present in the materials Nb_2PdSe_6, $Nb_2Pd_{0.71}Se_5$, and $Nb_3Pd_{0.72}Se_7$, respectively. The stoichiometry of the final two materials differs from their layer formulations since there are additional Pd atoms between the layers (vide supra). The layers constitute the set of composition $^2_\infty[Nb_{2n}PdSe_{4n+2}]$, n = 1, 2, 3, where the progression in composition of the layers is easily formulated as

$$^2_\infty[Nb_2PdSe_6] + 2\,^1_\infty[NbSe_2] = {}^2_\infty[Nb_4PdSe_{10}]$$

$$^2_\infty[Nb_4PdSe_{10}] + 2\,^1_\infty[NbSe_2] = 2\,^2_\infty[Nb_6PdSe_{14}]$$

The set is sketched in Figure 4, where the three-dimensional nature of the materials is emphasized. Similar to the preceding description of the layer $^2_\infty[Nb_6PdSe_{14}]$ as a collocation of the units $^1_\infty[Nb_6PdSe_{14}]$, the layers $^2_\infty[Nb_2PdSe_6]$ and $^2_\infty[Nb_4PdSe_{10}]$ may be described as a collocation of the simpler units $^1_\infty[Nb_2PdSe_6]$ and $^1_\infty[Nb_4PdSe_{10}]$, respectively. As before, these units may also be further subdivided into a set of crystallographically independent chains. Detailed descriptions of this procedure have been given elsewhere.[13b,c] Here we will concentrate on using the fundamental

(18) Grønvold, F.; Røst, E. *Acta Crystallogr.* **1957**, *10*, 329–331.

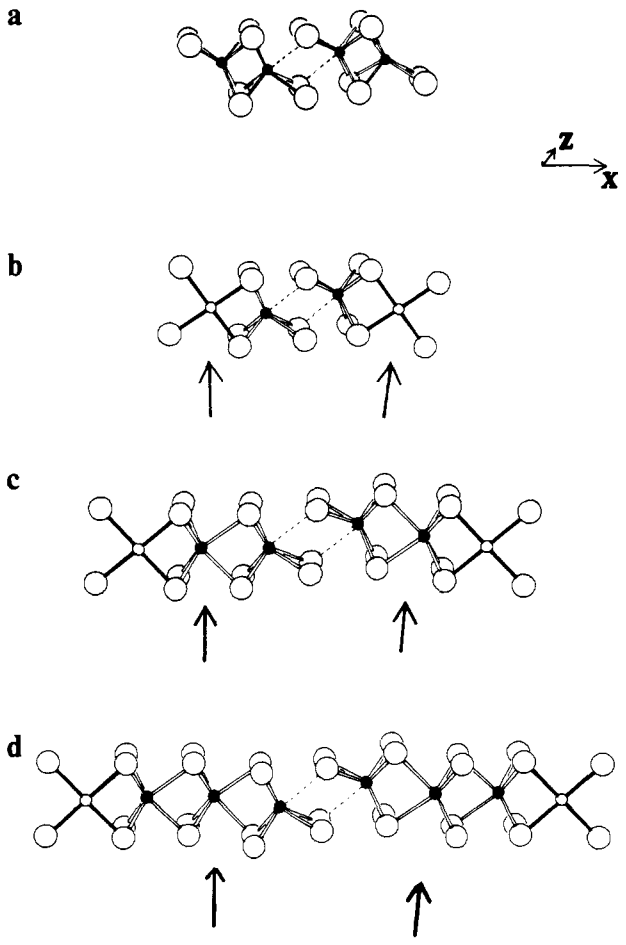

Figure 5. (a) $^1_\infty[NbAs_2]$ blocks. Nb atoms are small filled circles; As atoms are large open circles. (b) Section of the layer $^2_\infty[Nb_2PdSe_6]$ with arrows indicating point of insertion for Pd atoms. Nb atoms are small filled circles; Pd atoms are small open circles; Se atoms are large open circles. (c) Section of the layer $^2_\infty[Nb_4PdSe_{10}]$ with arrows indicating points of insertion of $^1_\infty[NbSe_2]$ blocks. (d) Section of the layer $^2_\infty[Nb_6PdSe_{14}]$ with arrows indicating points of insertion of $^1_\infty[NbSe_2]$ blocks.

units and their building blocks to demonstrate the progression in composition and the associated structural developments as they relate to the full three-dimensional structures.

These structural developments are diagrammatically depicted in Figure 5. In this figure are drawn sections of the layers that emphasize the juxtaposed nature of the fundamental units; the complete layers result from translations along the indicated directions (x, z). In the following discussion, all one-dimensional units result from translation in the direction z (see Figure 4). Two blocks of $^1_\infty[NbAs_2]$ present in the phase $NbAs_2$ are shown in Figure 5a. Each block consists of two trigonal prisms sharing a quadrilateral face; the prisms share triangular faces along the translational direction z. The blocks are juxtaposed in a manner similar to that described for the collocated units $^1_\infty[Nb_6PdSe_{14}]$ in the layer of $^2_\infty[Nb_6PdSe_{14}]$. To develop the structures of the layered chalcogenides through consideration of these geometrical units serves to link the topological similarities of the chalcogenides and those rare-earth-rich alloys that may also be described in a similar manner by association of the units $^1_\infty[NbAs_2]$.[19] If the blocks $^1_\infty[NbAs_2]$ are sliced along the common quadrilateral faces and a cube is inserted in the scission, the layer $^2_\infty[Nb_2PdSe_6]$ is geometrically produced (Figure 5b). The cube is represented by the enclosure of two face-to-face square planes centered by Pd atoms; these square planes are parallel to the triangular faces of the adjacent monocapped trigonal prisms. The layer $^2_\infty[Nb_4PdSe_{10}]$ is obtained from the layer $^2_\infty[Nb_2PdSe_6]$ by insertion of two units of $^1_\infty[NbSe_2]$. The edges common to the square planes and monocapped prisms in the layer $^2_\infty[Nb_2PdSe_6]$ are sliced and the $^1_\infty[NbSe_2]$ units are inserted. The results are emphasized by the arrows in Figure 5c. The triangular faces of the trigonal prism adjacent to the Pd-centered square are now orthogonal to this plane. This structural feature and the formal electronic reduction of the layers that results from inclusion of the units $^1_\infty[NbSe_2]$ will be discussed below. The process of inserting these units is repeated to afford the layers $^2_\infty[Nb_6PdSe_{14}]$ from $^2_\infty[Nb_4PdSe_{10}]$ (Figure 5d).

Within the set $^2_\infty[Nb_{2n}PdSe_{4n+2}]$ we have discovered examples with n = 1, 2, and 3. From consideration of the preceding structural developments, we speculate on the existence of new materials with larger values of n and further posit the inclusive set $^2_\infty[Nb_{n+1}PdSe_{2n+4}]$. The progression in composition for this set would be

$$^2_\infty[Nb_2PdSe_6] + 1^1_\infty[NbSe_2] = {}^2_\infty[Nb_3PdSe_8]?$$

$$^2_\infty[Nb_3PdSe_8] + 1^1_\infty[NbSe_2] = {}^2_\infty[Nb_4PdSe_{10}]$$

$$^2_\infty[Nb_4PdSe_{10}] + 1^1_\infty[NbSe_2] = {}^2_\infty[Nb_5PdSe_{12}]?$$

$$^2_\infty[Nb_5PdSe_{12}] + 1^1_\infty[NbSe_2] = {}^2_\infty[Nb_6PdSe_{14}]$$

$$^2_\infty[Nb_6PdSe_{14}] + 1^1_\infty[NbSe_2] = {}^2_\infty[Nb_7PdSe_{16}]?$$

The structural evolution of this set would proceed in a manner analogous to that of the set $^2_\infty[Nb_{2n}PdSe_{4n+2}]$ except the columns of Nb-centered edge-sharing trigonal prisms, $^1_\infty[NbSe_2]$, would be inserted singly. An ordered insertion of these units would result in loss of the inversion center between the juxtaposed columns of face-sharing $NbSe_3$ chains for those layers having an odd number of Nb atoms; this result is diagrammatically depicted in **1** for the hypothetical layer $^2_\infty[Nb_3PdSe_8]$. Such an ordered

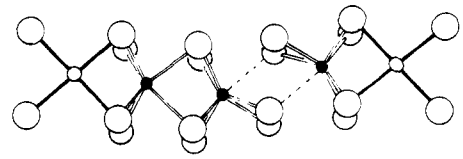

1

arrangement appears to be favored from consideration of the formation of pseudo-close-packed layers. New members in this set will probably be synthesized only under exacting conditions. The system Nb/Pd/Se has proved to be complex. The existence of several closely related compounds has made the preparation of single phases by simple heating difficult. The attainment of equilibrium appears to be hampered by the similar free energies of formation anticipated for the phases Nb_2PdSe_6, $Nb_2Pd_{0.71}Se_5$, $Nb_3Pd_{0.72}Se_7$, and other phases of similar composition.

Now that the structural interrelationships within the set $^2_\infty[Nb_{2n}PdSe_{4n+2}]$ have been described, we compare the geometrical aspects of this set with the well-studied binary layered chalcogenides $NbSe_3$ and $NbSe_2$ and some of their ternary derivatives. The phase $NbSe_3$ is composed of juxtaposed columns of formula $^1_\infty[NbSe_3]$ that form from face-sharing Se trigonal prisms occupied by Nb atoms, **2**. These columns may be bridged by geminate columns of octahedra to form the materials of the

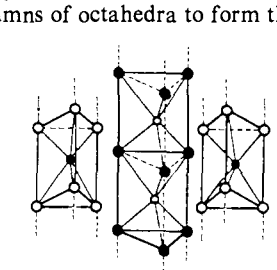

2

Nb_3FeSe_{10} structural type[20] or linked directly by square planes

(19) (a) LeRoy, J.; Moreau, J. M.; Paccard, D.; Parthé, E. *Acta Crystallogr. B* **1977**, *33*, 2414–2417. (b) LeRoy, J.; Moreau, J. M.; Paccard, D.; Parthé, E. *Acta Crystallogr. B* **1977**, *33*, 3406–3409.

to form the phase Nb_2PdSe_6[13b] (Figure 4). The geometrical analogues of these chains are also retained in the layers $^2_\infty[Nb_4PdSe_{10}]$ and $^2_\infty[Nb_6PdSe_{14}]$. For the compounds $NbSe_3$ and Nb_3FeSe_{10} the $NbSe_6$ prisms are somewhat irregular; some prisms contain short Se–Se distances, 2.34 Å, that are indicative of Se–Se bonding. The shortest intralayer Se–Se distances in Ta_2PdSe_6, $Nb_2Pd_{0.71}Se_5$, and $Nb_3Pd_{0.72}Se_7$ are 3.132 (4), 3.131 (1), and 3.126 (2) Å, respectively, and thus there is no indication of Se–Se bonding in these materials. In addition to absence of Se–Se bonding in the present materials, collocation of the $^1_\infty[NbSe_3]$ chains affords a seven-coordinate, monocapped, trigonal-prismatic environment of chalcogen atoms about the Nb atoms rather than the bicapped trigonal-prismatic environment observed in the materials $NbSe_3$ and Nb_3FeSe_{10}. Thus while the chains $NbSe_3$ of the layers $^2_\infty[Nb_{2n}PdSe_{4n+2}]$ are geometrically similar to those of other materials, the structural details are new and different.

The geometrical similarities between the phase $NbSe_2$ and the layers $^2_\infty[Nb_4PdSe_{10}]$ and especially $^2_\infty[Nb_6PdSe_{14}]$ may be inferred from our structural developments where chains of composition $^1_\infty[NbSe_2]$ were inserted. Each layer of the phase $NbSe_2$, **3**, may be viewed as a two-dimensional association of these chains

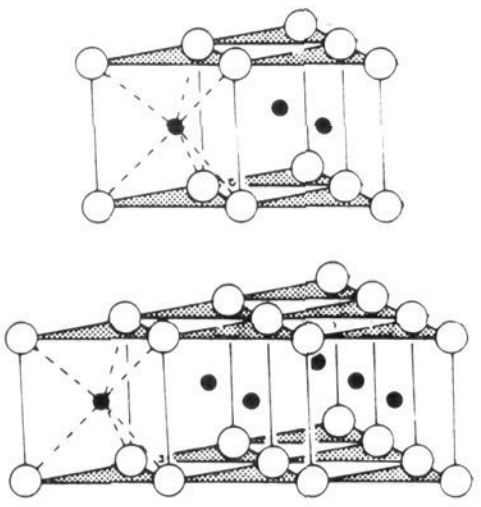

3

$^1_\infty[NbSe_2]$ or $NbSe_6$ prisms. Indeed the environment of nearest neighbors of atom Nb(2) in the compound $Nb_3Pd_{0.72}Se_7$ compares with that observed for the Nb atom of $NbSe_2$. As noted previously, the trigonal prisms of the present ternary materials are nearly regular although still more distorted than those observed in the more symmetrical compound $NbSe_2$. The structures of the layers $^2_\infty[Nb_{2n}PdSe_{4n+2}]$ may then be viewed as having structural elements derived from the phases $NbSe_3$ and $NbSe_2$ or both with new structural features that result from inclusion of Pd atoms.

The comparisons in structure of these laminar compounds also extend to the nature of the van der Waals' gap. As shown in Figure 6 for the phase $NbSe_2$ the sites between the layers consist of tetrahedra and octahedra. The tetrahedra are formed from three vertices in one layer and one vertex in the adjoining layer and hence point "up" or "down". The octahedra form a two-dimensional array by edge-sharing. The Se···Se distance across the gap is 3.52 Å. As shown in Figure 7, the gap of Ta_2PdSe_6 is made up of various tetrahedral, square-pyramidal, and octahedral sites. The tetrahedra are of two types: three vertices in a given layer with one in the adjacent layer as in $NbSe_2$ and two vertices from each layer. Between the latter type of polyhedra are located the square-pyramidal sites (Figure 7). The octahedral sites share edges, forming one-dimensional chains. The Se···Se distances across the gap range from 3.649 (3) to 4.071 (3) Å and are considerably longer than the value observed in the phase $NbSe_2$. As the blocks $^1_\infty[NbSe_2]$ are inserted, the van der Waals' gap adopts a nature similar to the layered dichalcogenides (Figures

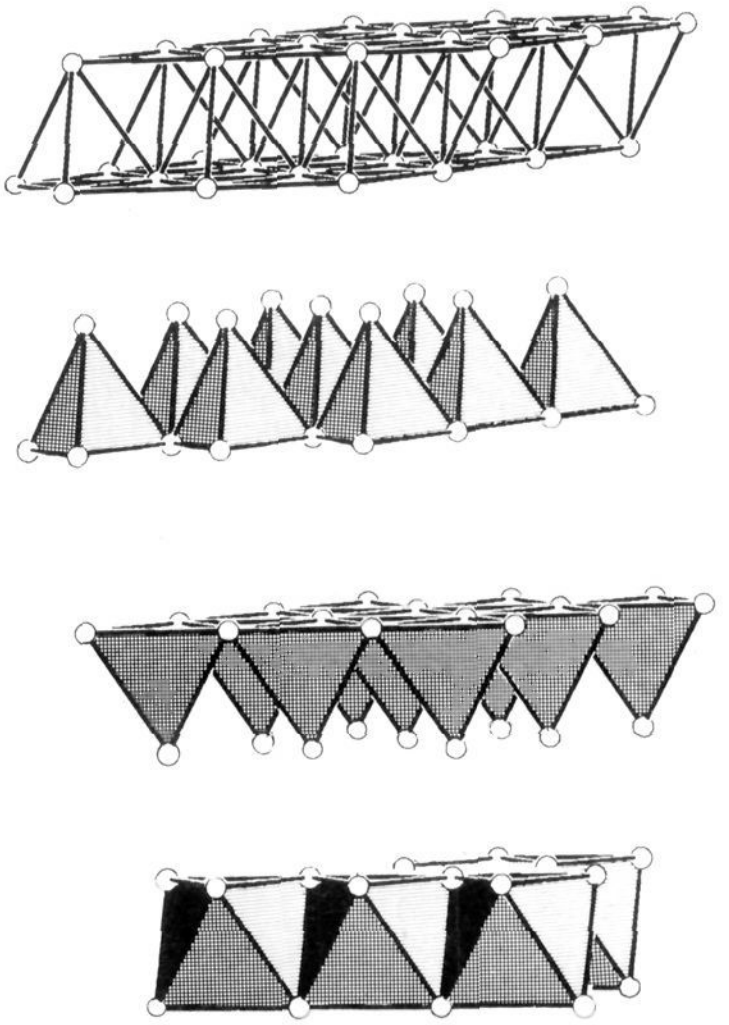

Figure 6. Illustration of the van der Waals' gap of the phase $NbSe_2$. The nature of the gap, tetrahedra that point "up", tetrahedra that point "down", and octahedra are depicted, respectively.

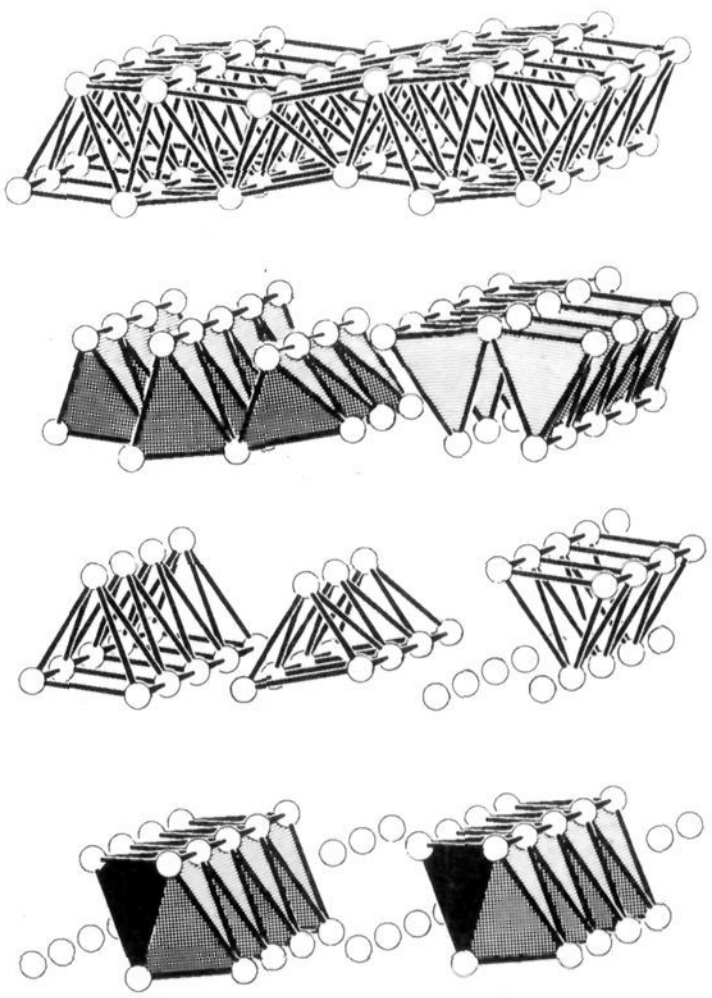

Figure 7. Illustration of the van der Waals' gap of the phase Ta_2PdSe_6. The nature of the gap, tetrahedra, square pyramids, and octahedra are depicted, respectively.

8 and 9) in which tetrahedra that point "up" and "down" and similar octahedral sites become prevalent. Not only is the comparison qualitative but the size of these sites also parallels those of the dichalcogenides. As seen from Table VI, as the $^1_\infty[NbSe_2]$ blocks are inserted and the complexity of the layer increases the sites become more regular and resemble more closely those of the phase $NbSe_2$. The distinguishing feature of these gaps, however, is the presence of the rhombic site (Figures 8 and 9). This site,

(20) (a) Hillenius, S. J.; Coleman, R. V.; Fleming, R. M.; Cava, R. J. *Phys. Rev. B* **1981**, *23*, 1567–1575. (b) Cava, R. J.; Himes, V. L.; Mighell, A. D.; Roth, R. S. *Phys. Rev. B* **1981**, *24*, 3634–3637. (c) Meerschaut, A.; Gressier, P.; Guemas, L.; Rouxel, J. *Mater. Res. Bull.* **1981**, *16*, 1035–1040. (d) Salem, A. B.; Meerschaut, A.; Guemas, L.; Rouxel, J. *Mater. Res. Bull.* **1982**, *17*, 1071–1079. (e) Wertheim, G. K.; DiSalvo, F. J.; Buchanan, D. N. E. *Phys. Rev. B: Condens. Matter* **1983**, *28*, 3335–3338.

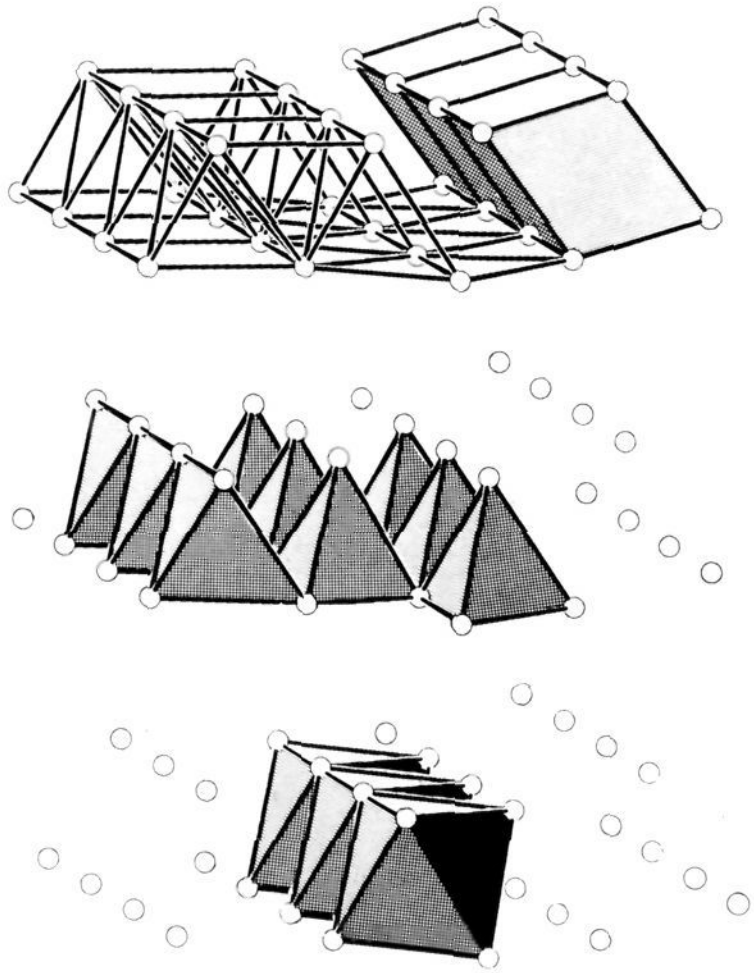

Figure 8. Illustration of the van der Waals' gap of the phase $Nb_2Pd_{0.71}Se_5$. The nature of the gap with the rhombic prism, tetrahedra, and octahedra are depicted, respectively.

Table VI. Distances (Å) in van der Waals' Gap from Center of Vacant Sites to Their Vertices for Selected Materials

compound	tetrahedra	octahedra	square pyramid
R–$NbSe_2$[a]	2.12	2.47	
Ta_2PdSe_6	1.96–2.58	2.49–2.76	2.06–2.54
$Nb_2Pd_{0.71}Se_5$	2.09–2.22[b]	2.40–2.49	2.41–2.62
	2.01–2.59[c]		
$Nb_3Pd_{0.72}Se_7$	2.11–2.25[b]	2.40–2.51	2.36–2.60
	2.06–2.50[c]		

[a] See ref 3b. [b] One vertex in "lower" layer and three vertices in "upper" layer. [c] Two vertices in "lower" layer and two vertices in "upper" layer.

easily described as two trigonal prisms sharing a quadrilateral face, provides new possibilities for chemical modification; in the present instance it is occupied to 43% by Pd atoms.

The channel-type structure of the phase $Nb_2Pd_3Se_8$ and the layered-type structure of $Co_2Ta_4PdSe_{12}$ are two additional compounds that form with new combinations of polyhedra similar to those of the set $^2_\infty[Nb_{2n}PdSe_{4n+2}]$. The relationship between the layers $^2_\infty[Nb_4PdSe_{10}]$ and the compound $Nb_2Pd_3Se_8$ is demonstrated in Figure 10. Although this polyhedral derivation of the phase $Nb_2Pd_3Se_8$ from the layers $^2_\infty[Nb_4PdSe_{10}]$ is artificial, it aids in the establishment of the structural relationships among these materials, provides us with an alternative polyhedral arrangement for the phase $Nb_2Pd_3Se_8$, and leads naturally to the structural type $Co_2Ta_4PdSe_{12}$. As shown in Figure 10b the layers $^2_\infty[Nb_4PdSe_{10}]$ may be modified by substitution of Pd atoms for two $^1_\infty[NbSe]$ units. This substitution affords the basic structural units observed in the compound $Nb_2Pd_3Se_8$. These units could coalesce along the indicated dashed lines to form a layered compound having Pd atoms in a five-coordinate square-pyramidal environment of Se atoms. The association of the square pyramids that would result for this compound is known for molecular compounds.[21] However, these layers are not observed. Rather, as shown in Figure 10, the structural units must be translated and rotated to produce the observed structure. This structure also has one of the Pd atoms in a square-pyramidal environment. Return now to the units of

(21) Ross, F. K.; Stucky, G. D. *J. Am. Chem. Soc.* **1970**, *92*, 4538–4544.

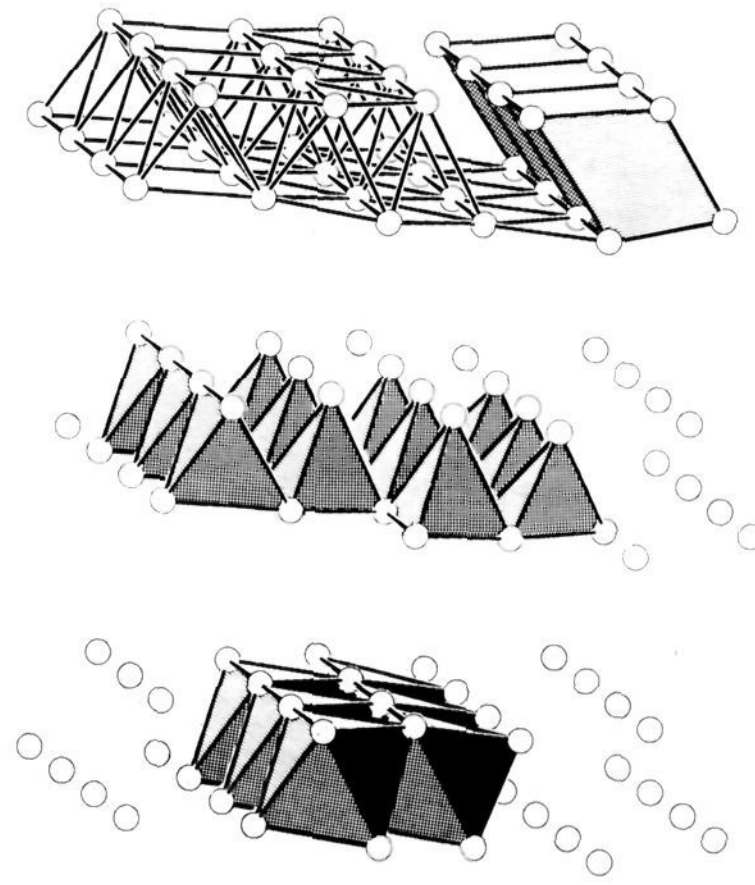

Figure 9. Illustration of the van der Waals' gap of the phase $Nb_3Pd_{0.72}Se_7$. The nature of the gap with the rhombic prism, tetrahedra, and octahedra are depicted, respectively.

Table VII. Parsimony Indices[a] $I_t = 1 - e/t$ and $I_c = 1 - e/c$ and Density of Packing, D, Se Spheres for Selected Chalcogenides

	t^b	c^c	e^d	I_t	I_c	D^e
Nb_2PdSe_6	4	5	3	0.25	0.40	0.33
$Nb_2Pd_{0.71}Se_5$	7	9	3	0.57	0.66	0.33
$Nb_3Pd_{0.72}Se_7$	8	12	3	0.63	0.75	0.33
$Nb_2Pd_3Se_8$	5	7	3	0.40	0.57	0.30
$Co_2Ta_4PdSe_{12}$	9	10	4	0.56	0.60	0.34
$NbSe_2$	2	2	2	0	0	0.33

[a] Reference 21. [b] Number of topologically distinct species. [c] Number of crystallographically different constituents. [d] Number of different chemical elements. [e] The densities of packing are derived from a radius of 1.70 Å for the Se atom.

Figure 10a. Insertion of a metal-centered bioctahedral chain of Se atoms between these units produces the topology of the phase $Co_2Ta_4PdSe_{12}$ (Figure 11). In this material, with its intriguing collection of polyhedra, the Co atoms occupy the square-pyramidal sites, the Pd atoms occupy the square-planar sites, and the Ta atoms occupy both the trigonal prismatic and octahedral sites.

We conclude this section with a general consideration of the structural complexity and the packing densities of these chalcogenides. In Table VII for each of the compounds are given the parsimony indices I_t and I_c[22] and the fraction of total space occupied by the packing of Se spheres of equal radius. The parsimony indices I_t and I_c are a measure of the topologic and crystallographic complexity, respectively, of a given structural type. Parsimonius structures have indices $0 \leq I \leq 0.33$ and lavish structures have indices $I \geq 0.66$. The simple binary phase $NbSe_2$ has limiting indices and is parsimonius. Similarly, the phase Nb_2PdSe_6 is simple and topologically parsimonius. With the exception of the value 0.75 for the index I_c of the phase $Nb_3Pd_{0.72}Se_7$, the indices for the remaining phases reveal an intermediate complexity. The densities of packing are equal for each of the compounds. These densities may be compared with the values 0.34 and 0.70 observed for diamond and body-centered cubic packings, respectively. The small values for the densities of the chalcogenides reflect the open coordination environments of the metal atoms and the presence of van der Waals' gaps. Consideration of the limited lavishness of the ternary Pd chal-

(22) Baur, W. H.; Tillmanns, E.; Hofmeister, W. *Acta Crystallogr. B* **1983**, *39*, 669–674.

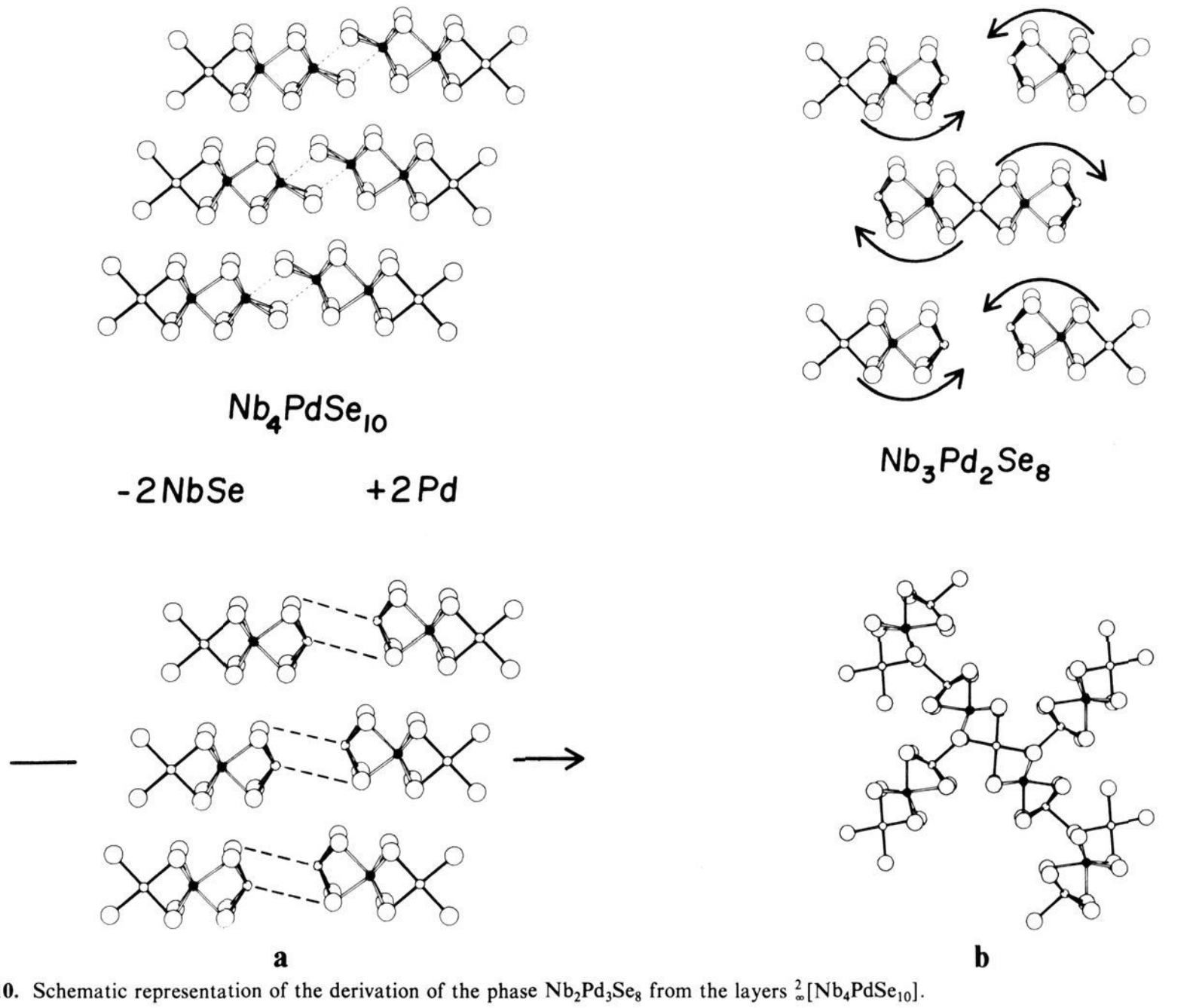

Figure 10. Schematic representation of the derivation of the phase $Nb_2Pd_3Se_8$ from the layers $^2_\infty[Nb_4PdSe_{10}]$.

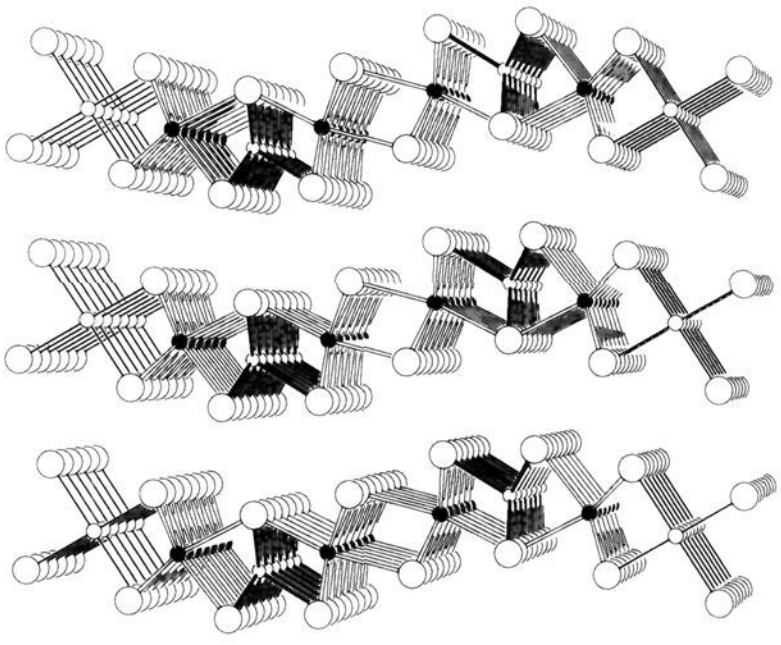

Figure 11. Perspective view of the structure of $Co_2Ta_4PdSe_{12}$. Co atoms are small open circles with shaded bonds; Ta atoms are small filled circles; Pd atoms are small open circles; Se atoms are large open circles.

cogenides and their similar packing densities as compared with the phase $NbSe_2$ provides an illustration of efficacy for the structural association of Pd-centered square planes and Nb-centered trigonal prisms—a result to have been anticipated from the metrical details of binary Pd and Nb chalcogenides and the topological aspects of associating cubes and trigonal prisms.[23]

Electronic Nature of the Ternary Laminar Pd Chalcogenides

The electrical conductivity in these Pd chalcogenides ranges from semiconducting to metallic.[13] From this behavior and our structural and chemical results we formulate a simple model for the electronic structure of these materials.

Note that the Se···Se distances in each of these layered materials are greater than 3.1 Å. This value may be compared with the Se···Se distance 4.0 Å in the phases $Ba_3Fe_3Se_7$[24] and $MgAl_2Se_4$[25] and the Se–Se distance 2.3 Å generally associated with a Se–Se single bond. If the distance 4.0 Å corresponds to Se^{II-}···Se^{II-} van der Waals' contacts and the distances 2.3 Å to a Se–Se single bond, as in Se_2^{II-}, the intermediate value 3.1 Å is difficult to describe. Indeed, similar distances in other transition-metal chalcogenides have been discussed previously in various contexts.[26] We believe the intermediate Se···Se distances result from a stabilization of the Se orbitals by their interaction with transition-metal orbitals; there is a substantial covalent contribution to the metal-to-chalcogen bonding, and this bonding determines the metrical results. We anticipate no Se–Se bonding in these materials and assign to the Se atoms the formal oxidation state Se^{II-}.

We next assign to the Pd atoms the formal oxidation state Pd^{II}. This assignment is not unique for the complete series of materials but merely reflects our preference and experience. With these assignments the valence description Nb^V, Pd^{II}, and Se^{II-} obtains for the materials $Nb_2Pd_3Se_8$ and Nb_2PdSe_6. From the electronegativity of the atoms and this valence description, the electronic levels would be ordered Se < Pd < Nb. As these materials are semiconductors, a small energy gap could be anticipated to occur between the filled levels of d^8 Pd^{II} and the empty levels of d^0 Nb^V. Extending the description to the materials $Nb_2Pd_{0.71}Se_5$ and

(23) Nyman, H. *J. Solid State Chem.* **1976**, *17*, 75–78.

(24) Hong, H. Y.; Steinfink, H. *J. Solid State Chem.* **1972**, *5*, 93–104.
(25) Dotzel, P.; Schäfer, H.; Schön, G. *Z. Anorg. Allg. Chem.* **1976**, *426*, 260–268.
(26) (a) Shannon, R. D.; Vincent, H. *Struct. Bonding* **1974**, *19*, 1–43. (b) Gamble, F. R. *J. Solid State Chem.* **1974**, *9*, 358–367. (c) Shannon, R. D. *Acta Crystallogr. A* **1976**, *32*, 751–767.

$Nb_3Pd_{0.72}Se_7$ we obtain the strict valence descriptions $Nb^{4.3}$, Pd^{II}, Se^{II-}, and $Nb^{4.2}$, Pd^{II}, Se^{II-}, respectively. As indicated by the valence description for these materials, the additional electrons are probably transferred into bands with substantial Nb character. The partial filling of these bands affords the metallic behavior for $Nb_2Pd_{0.71}Se_5$.[13b]

The electronic structure of these materials may then be viewed as similar to that formulated for the layered compounds $NbSe_3$[27] and $NbSe_2$.[28] For these phases the electronic states at the Fermi level are mostly of metal d character; their dispersion derives in part from through-space metal-to-metal interactions. Below these levels are mostly filled Se states. As demonstrated by analysis of the results of various calculations,[28,29] the detailed nature of the Nb d bands is not readily defined by crystal-field arguments. Nevertheless, the d bands are only partially occupied, which results in the observed metallic behavior. A similar result is anticipated for the ternary Pd chalcogenides. As the Nb–Nb distances in these materials are similar to those of the phases $NbSe_3$ and $NbSe_2$, similar dispersion of the Nb d bands is expected. From our partially ionic model, these d bands are placed above filled Pd and Se states. From the number of electrons in the phases $Nb_2Pd_{0.71}Se_5$ and $Nb_3Pd_{0.72}Se_7$, the bands of predominantly Nb d character are partially filled, affording metallic behavior.

An additional consequence of the presence of partially filled d bands in the phases $NbSe_3$ and $NbSe_2$ is the ability of these compounds to accept various electron-donating species, such as Li atoms or additional transition metals between their layers. Charge is transferred from these donors into the partially occupied Nb d bands. That such an intercalation chemistry may also be anticipated for the ternary Pd materials may be inferred from our recent experiments on the system Ta/Pd/S. The material $Ta_2Pd_{0.89}S_5$ has been prepared.[30] This compound has layers $^2_\infty[Ta_4PdS_{10}]$ analogous to those of $^2_\infty[Nb_4PdSe_{10}]$ that occur in the phase $Nb_2Pd_{0.71}Se_5$, but the Ta analogue has a higher concentration of Pd atoms between the layers. This behavior then parallels the insertion chemistry of the binary layered chalcogenides.

In our model we have neglected the details of the Nb–Pd and Nb–Nb interactions and the possible anisotropy of the electrical conductivity within a given layer. These topics will be discussed in a future report on the analysis of tight-binding band structure calculations.[31]

In sum, we have presented results on a class of new and developing materials. While some of the results may be interpreted as for other layered compounds, others present us with new features and opportunities. The arrangements of square planes and trigonal prisms have themselves provided a new experimental structural chemistry. The variety of metal-to-metal interactions and electron counts possible in these compounds may afford unusual electrical characteristics. Here the preparation and study of the pristine laminar compounds Nb_4PdSe_{10} and Nb_6PdSe_{14} appears especially interesting. The new association of polyhedra in the matrials described here provides a selectivity in chemical modification unprecedented in other materials. This is demonstrated by the nonstoichiometric insertion of Pd atoms in the rhombic site between the layers. In general, selectivity arises from the stereochemical preferences of the metal atoms and extends to the variety of vacant sites present in these new materials.

Acknowledgment. This research was supported by the U.S. National Science Foundation—Solid State Chemistry—Grant No. DMR83-15554. Use was made of the Scanning Electron Microscope Facility of Northwestern University's Material Research Center, supported in part under the NSF-MRL program (Grant DMR82-16972).

Registry No. $Nb_3Pd_{0.72}Se_7$, 96477-43-9.

Supplementary Material Available: Anisotropic thermal parameters (Table III) and structure amplitudes (×5) (Table IV) (13 pages). Ordering information is given on any current masthead page.

(27) (a) Bullet, D. W. *J. Phys. C* **1979**, *12*, 277–281. (b) Bullet, D. W. *Solid State Commun.* **1978**, *26*, 563–565. (c) Hoffmann, R.; Shaik, S.; Scott, J. C.; Whangbo, M.-H.; Foshee, M. J. *J. Solid State Chem.* **1980**, *34*, 263–269. (d) Whangbo, M. H.; Gressier, P. *Inorg. Chem.* **1984**, *23*, 1305–1306.

(28) (a) Mattheiss, L. F. *Phys. Rev. B* **1973**, *8*, 3719–3740. (b) Fong, C. Y.; Cohen, M. L. *Phys. Rev. Lett.* **1974**, *32*, 720–724. (c) Kertesz, M.; Hoffmann, R. *J. Am. Chem. Soc.* **1984**, *106*, 3453–3460.

(29) Fong, C. Y.; Schlüter, M. In "Physics and Chemistry of Materials with Layered Structures", Wieting, T. J., Schlüter, M., Eds.; d. Reidel Publishing Co.: Dordrecht, 1979; pp 145–315.

(30) Squattrito, P. J.; Ibers, J. A., unpublished results.

(31) Keszler, D. A.; Hoffmann, R., manuscript in preparation.